scientific reports



OPEN

Preparation and characterization of niosomes containing silver nanoparticles as a radiosensitizer for enhancing radiotherapy of the lung cancer

Hossein Danafar^{1,3,4⊠}, Mahdi Nayyeri Maleki¹, Amir Hosein Moradi², Ali Sharafi³ & Kayvan Nedaei³

Lung cancer was associated with a high mortality rate. However, the critical challenges in radiotherapy are enhancing tumor damage and minimize the side effects to the healthy tissues. A strategic approach to overcome this challenge includes using different radiosensitizer to increase the efficiency of radiotherapy while reducing side effects on normal tissues. Significant progress has been achieved in the development of materials based on nanotechnology. Nanomaterial-based radiosensitizers increase the tumor cells sensitivity to ionizing radiation, and accelerating DNA damage through the production of free radicals. Therefore, in the present study, the radio sensitization efficiency of silver nanoparticles-loaded niosomes for the treatment of lung cancer has been investigated. Silver nanoparticles synthesis protocol was based on the chemical reduction method and then they were loaded inside niosomes using the thin layer hydration method. The physical and chemical characteristics of the designed nanosystems were evaluated using different instrumental and laboratory methods, including FT-IR, UV-Vis, DLS, FE-SEM, EDAX techniques. To investigate the cytotoxicity of prepared nanosystems, the MTT assay was used against two cell lines, including normal human lung cells (MRC-5) and lung cancer cells (A549), in the absence and presence of radiotherapy rays. The size and poly dispersity index of the resulting nanoparticles are in the range of Nano scale and are suitable for cancer studies. The morphology of the resulting nanoparticles was found to be spherical and homogeneous. The structural and optical analysis of the nanoparticles showed the successful synthesis of niosomes containing silver nanoparticles. Also, the EDAX technique confirmed the presence of silver nanoparticles inside niosomal formulations. The encapsulation efficiency of silver nanoparticles was 49.9% ± 0.40 for silver nanoparticles. In the following, the biocompatibility of the formulation prepared using the MTT method toward the normal cell line MRC-5 showed that no significant toxicity in the studied concentrations. MTT test toward the A549 lung cancer cell line showed an increase in the toxicity of radiotherapy in lung cancer. Our study showed that silver nanoparticles-loaded niosomal nanosystems possess significant therapeutic efficacy radiotherapy of the lung cancer. On the other hand, loading silver nanoparticles inside niosomal carriers reduced the toxicity of silver nanoparticles and introduced them as a suitable option for cell experiments. Also, we showed that the synthesized formulations in combination with radiotherapy increase the efficiency treatment through its synergistic effect.

Keywords Silver nanoparticles, Niosome, Lung Cancer, Radiotherapy, Radiosensitizer

¹Pharmaceutical Nanotechnology Research Center, Faculty of Pharmacy, Zanjan University of Medical Sciences, Zanjan, Iran. ²Student Research Committee, School of medicine, Zanjan University of Medical Sciences, Zanjan, Iran. ³Pharmaceutical Biotechnology Research Center, Faculty of Pharmacy, Zanjan University of Medical Sciences, Zanjan, Iran. ⁴Department of Medicinal Chemistry School of Pharmacy, Zanjan University of Medical Sciences, Zanjan 45139-56184, Iran. [⊠]email: danafar@zums.ac.ir

Abbreviations

SCLC Small cell lung carcinoma
NSCLC Non-small cell lung carcinoma
IBRT Internal beam radiation therapy
EBRT External beam radiation therapy
RBN Nanomaterial-based radiosensitizers
EPR Enhanced permeability and retention effect

AgNPs Silver nanoparticles
ROS Reactive oxygen species
FBS Fetal bovine serum

DMEM Dulbecco's modified eagle medium

DMSO Dimethyl sulfoxide
DLS Dynamic light scattering

FT-IR Fourier-transform infrared spectroscopy

UV-Vis Ultraviolet-visible

FE-SEM Field emission scanning electron microscope ICP-MS Inductively coupled plasma mass spectrometry

XRD X-ray diffractometer EDX Energy dispersive X-ray

Cancer represents a significant public health concern and constitutes one of the principal causes of mortality globally. In this context, lung cancer emerges as the predominant contributor to cancer-related fatalities. In the year 2022, approximately 2.4 million individuals received a diagnosis of lung cancer, while an estimated 1.8 million individuals succumbed to this malignancy. Lung cancer is classified into small cell lung carcinoma (SCLC) and non-small cell lung carcinoma (NSCLC)¹. These two groups of lung cancers have different characteristics. The diagnosis of each of them is essential to guide the treatment. Also, cancer diagnosis in early stages is very important and the advances made in this field have made it possible to identify and treat cancer in the early stages. However, the existing methods still cannot fully provide the sensitivity and specificity required for accurate cancer diagnosis. Several risk factors have been proved that could be participating in the pathogenesis of the lung cancer². These risk factors include: smoking, cooking smoke, asbestosis, different chemical substances at work, diet, familial history and, genetics. The different types of the treatment have proposed for lung cancer as monotherapy and combined therapy. Surgery, chemotherapy, radiotherapy and targeted therapy (such as immunotherapy) are the different treatments that have been utilized³⁻⁵. Meanwhile, radiotherapy is a valuable treatment in lung cancer. Radiotherapy for SCLC and non-operable and non-metastatic cancers has been used for many years. On the other way, radiotherapy accounts for 35% of all NSCLC cancers in locally advanced stages. Also, this method can be used as an adjuvant treatment after surgery and could utilize in metastatic disease reduce pain and symptoms. Thus, Radiotherapy is one of the main treatment methods for lung cancer and is effective for about half of lung cancer patients. The radiotherapy mainly plays its role through the direct and indirect pathways. The direct pathway is instigated by the immediate radiation interaction with organic molecules, resulting in the free radical's generation and subsequent DNA fragmentation. The indirect pathway is predominantly facilitated by the ionization of water within human biological tissues. Radiotherapy has been performed in two main pathways: Internal Beam Radiation Therapy (IBRT) and External Beam Radiation Therapy (EBRT). Tumor resistance to radiotherapy may lead to a decrease in its effectiveness, and result in tumor recurrence and metastasis. Therefore, it is necessary to investigate the molecular mechanisms that are responsible for the development of radiation therapy resistance and to discover new therapeutic targets to overcome this resistance. A better understanding of these mechanisms can lead to the targeting of therapeutic agents to counter tumor resistance, the development of new antitumor targets, and the development of therapeutic strategies to re-sensitize cancer cells to therapy^{6,7}. Radiosensitizers provided new opportunities for radiotherapy to treat cancer. They increase the sensitivity of cells to radiotherapy. These compounds or agents can directly increase the harmful effects of radiotherapy on cancer cells or stimulate mechanisms that lead to the growth retardation of cancer cells in response to radiation. Thus, these materials and methods increase the radiation sensitivity of tumor8. They could also reduce the adverse effects of radiotherapy to normal tissue and, radiation dose. Several radiosensitizers include chemotherapeutic drugs, angiogenesis inhibitors, cell proliferator inhibitors, apoptosis inducer agents and, nanomaterial-based radiosensitizers. In this context, Nanomaterial-Based Radiosensitizers (RBN) enhance the sensitivity and reactivity of neoplastic cells to ionizing radiation, thereby promoting the generation of free radicals and expediting DNA damage. RBNs have garnered significant scholarly attention owing to their remarkable physicochemical characteristics, including inherent radiosensitivity, substantial drug loading capacity, commendable biocompatibility, and proficient tumor-targeting efficacy, augmented by the Enhanced Permeability and Retention effect (EPR)9. Utilizing of the nanoparticles with high atomic number in radiotherapy has received a lot of attention. Nanomaterials with elements with high atomic numbers such as bismuth (Bi), gold (Au) and silver (Ag) are used as dose enhancers due to their ability to strongly absorb photons and increase radiation deposition for radiotherapy. The X-ray absorption characteristics of the primary material are employed to enhance the availability of the absorption cross-section, focus the energy of the high-energy beam, elevate the generation of free radicals, directly augment DNA damage, and consequently optimize the efficacy of radiotherapy. Conversely, radiosensitizers have the potential to amplify the susceptibility of tumor cells to radiation through the reactive oxygen species generation, modulation of the cell cycle, enhancement of intrinsic cellular hypoxia, inhibition of DNA repair mechanisms, suppression of tumor angiogenesis, and inhibition of cellular auto-activation¹⁰. Due to remarkable advances in nanotechnology, various nanomaterials have been designed to increase the effectiveness of radiotherapy. Silver and gold nanoparticles have attracted

special attention due to their excellent radiosensitizer properties. The application of silver nanoparticles (AgNPs) as a radiosensitizer has attracted wide attention in recent years. AgNPs have radiosensitizing properties like gold nanoparticles. Compared to gold nanoparticles, the cost of silver nanoparticles is relatively lower and therefore they are economical in terms of cost. It has been established through empirical evidence that AgNPs enhance oxidative stress within neoplastic cells, disrupt cellular membranes, and precipitate apoptotic processes. The underlying mechanism of radiosensitization associated with AgNPs entails the infiltration of Ag+ ions, which sequester electrons and induce oxidative injury in cellular structures, thereby augmenting the generation of reactive oxygen species (ROS) and diminishing intracellular adenosine triphosphate (ATP) levels¹¹. In this context, research has indicated that AgNPs may inhibit the proliferation of lung cancer cells via various antitumor signaling pathways^{12,13}. Recent investigations showed that AgNPs augment the capacity to enhance cellular sensitivity and integrity in response to radiotherapy. This modality of oncological intervention is predicated upon the intricate interactions between ionizing radiation (which encompasses gamma rays, X-ray photons, or charged particles) and biomolecular constituents for the purpose of eliminating malignant cells. The interaction between silver nanoparticles (AgNPs) and X-ray photons induces the liberation of electrons. These freed electrons interact directly with deoxyribonucleic acid (DNA), resulting in the induction of double-strand breaks, or they may ionize water molecules, thereby generating reactive oxygen species (ROS), which can lead to further cellular damage (including DNA lesions, lipid peroxidation, endoplasmic reticulum stress, and mitochondrial dysfunction), ultimately resulting in cellular demise¹⁴. Niosomes are defined as vesicular structures that comprise cholesterol and alkyl or dialkyl polyglycerol ether moieties. The structural composition of niosomes allows for the transfer of drug molecules with a broad spectrum of solubility, attributable to the presence of both lipophilic and hydrophilic components within their architecture. Such systems may serve as a viable alternative to conventional liposomal drug carriers¹⁵. Niosomes are regarded as a novel class of drug delivery systems for oncological therapies, as they facilitate the targeted administration of pharmaceuticals to malignant tissues while mitigating severe toxicological effects and enhancing drug stability. In this context, Kerr et al. synthesized niosomes encapsulating adriamycin and employed them for the treatment of lung carcinoma. The results obtained indicated that the therapeutic index of adriamycin was significantly augmented when delivered in the niosomal form¹⁶. Recent studies have demonstrated that combination therapies were also associated with better results than monotherapy in dealing with cancer. Due to this issue, the clinical research focused on the combination therapy and they supported that these methods will become the main treatment methods not only for cancer but also for many other diseases. It should be mentioned that the combination of radiotherapy with other treatment methods can reduce the dose of radiation energy and effectively eradicate cancer cells. Accordingly, the rational design of multifunctional Nano-platforms along with other innovative approaches is essential to achieve the combination therapy. Thus, in this study we prepared and characterized of noisomes containing AgNPs to evaluate that if they could act as a radiosensitizer and improve the lung cancer radiotherapy efficacy or not.

Materials & methods Material

Cholesterol, Tween 80, Span 80, chloroform, and acetone were procured from Merk Company (Germany). Methanol was acquired from Merk Company (Spain). Ethanol at a concentration of 96% was sourced from Kimiya Company (Iran). Silver nitrate (AgNO₃), MTT powder, and Dimethyl sulfoxide (DMSO) were obtained from Sigma-Aldrich Company (USA). Fetal Bovine Serum (FBS), Trypsin 25%, Trypan blue, and Dulbecco's Modified Eagle Medium (DMEM) were purchased from Gibco Company (USA) The MRC5 and A549 cells were procured from the Pasteur Institute of Iran, a renowned research institution in the Middle East.

Preparation of nanoparticles

First, AgNPs, plain niosomes and niosomes containing AgNPs were synthesized using the following methods.

AoNPs synthesis

The AgNPs synthesis was done by the Ferns method¹⁷. In this method, chemical reduction of AgNO₃ using a reducing agent such as sodium citrate is used. In the present project, first 50 mL of one molar AgNO₃ solution was prepared. The AgNO₃ solution was brought to boiling temperature about 100 °C (degrees Celsius). Then, the sodium citrate solution with the appropriate concentration (1% by weight) was added drop by drop to the boiling AgNO₃ solution. After adding sodium citrate, the solution was stirred for 40 min. In this step, AgNPs are formed and the color of the solution changed. The formed AgNPs were separated by centrifugation (1400 rpm for 10 min) and distilled water has used to wash in order to remove the remaining unreacted substances.

Niosomes synthesis

The synthesis of niosomes was done by the thin layer hydration method, which is a common and effective method for preparing this type of nano-carriers¹⁸. To reach this purpose, a mixture of 600 mg of Tween 80 and Span 80, as well as 80 mg of cholesterol was added to a spherical flask and dissolved by adding chloroform. Then, a rotary evaporator was used under vacuum conditions at a temperature of 50 °C to remove chloroform and produce a thin film. After that, the resulting thin layer was kept in a vacuum oven at a 50 °C of temperature for 2 h (h) and completely removes the solvent. To start the hydration of the thin layer, 10 mL of water was gradually added to the mixture and thoroughly stirred on a hot plate with the help of a magnetic stir bar in the flask. After that, sonication was performed for 10 min. Finally, the resulting niosomes named as were collected.

Synthesis of the niosomes containing AgNPs

A mixture of 600 mg of Tween 80 and Span 80 as well as 80 mg of cholesterol was added to a spherical flask and dissolved by adding chloroform. Then, a rotary evaporator was used under vacuum conditions at a 50 $^{\circ}$ C to remove chloroform and produce a thin layer. After that, the resulting thin layer was kept in a vacuum oven at a 50 $^{\circ}$ C for 2 h to remove the solvent completely. To start the hydration of the thin layer, 10 mL of water containing AgNPs was gradually added to the mixture and thoroughly stirred on a hot plate with the help of a magnetic stirrer rod in the flask. After that, sonication was performed for 10 min. Finally, niosomes containing AgNPs named as Nio-AgNPs were collected¹⁹.

Characterization

Characterization of physical and chemical properties of nanoparticles is a process in which various properties of nanoparticles, including size, shape, chemical composition, crystal structure, specific surface area, and surface properties are determined and analyzed. This process is important for several reasons and can be done in different ways.

Investigating the hydrodynamic size of nanoparticles

The dimensions and size distribution of AgNPs, and Nio-AgNPs were determined employing the Dynamic Light Scattering (DLS) methodology, with the results documented in a graphical format. The zeta potential of both the nanoparticle surface and the carriers was similarly evaluated utilizing the DLS apparatus. To facilitate this process, the initially prepared samples were diluted to attain the requisite absorption range suitable for DLS assessments, subsequently allowing for the determination of the dimensions of the prepared nanoparticles via the DLS device¹⁹.

Fourier transform infrared spectroscopy

The structural characteristics and composition of prepared nanoparticles were determined using Fourier-transform infrared spectroscopy (FT-IR) method. To perform this test, the desired samples were mixed with potassium bromide (KBr) inside the mortar. Then, using a hydraulic press, transparent tablets were prepared and then they were placed in the device and the corresponding spectra were recorded in the range of 500–4000 cm⁻¹.

Ultraviolet-visible (UV-Vis) spectrophotometry

The UV-Vis absorption spectrum of prepared nanoparticle solutions was recorded using UV-Vis spectroscopy. To do this, first, two quartz cells were selected as controls and placed in the device with the desired solvent. Then, one of the cells (related to the sample) was taken out and scanned by diluting the sample to obtain the maximum desired wavelength for the samples. The same method was used to read the absorbance of the samples, with the difference that when we obtained the maximum wavelength, instead of scanning the sample, we entered the maximum absorbance value and the absorbance of each value was recorded.

The field emission scanning Electron microscope (FE-SEM)

The morphological attributes of the synthesized nanoparticles were subjected to imaging and analysis utilizing the FE-SEM apparatus operating at a voltage of 15 kV. Additionally, the occurrence and distribution of carbon, nitrogen, oxygen, and silver atoms within the formulations were examined through Energy Dispersive X-ray (EDX) analysis.

The inductively coupled plasma mass spectrometry (ICP-MS)

The technique of ICP-MS was employed to quantify the concentration of AgNPs present in the formulations. To achieve this, three replicates of the synthesized formulations were introduced into the ICP-MS device, allowing for the measurement of AgNPs concentration in each formulation.

X-ray diffraction (XRD)

XRD patterns of AgNPs, niosomes and niosomes containing AgNPs were analysed using device with 40 kV and 45 mA setting. To do this, the samples were dried and their XRD patterns were recorded continuously in the 2θ range of 90-7 degrees with a scanning speed of 3.2 degrees per minute.

Encapsulation efficiency of AgNPs in niosomes

To measure the encapsulation efficiency of AgNPs inside niosomes, the amount of synthesized Ag was first determined using ICP-MS method. Then, 500 μ L of nanparticles were sampled and digestion and dilution steps were performed. Next, centrifugation was used to purify niosomes (suspensions containing nanoparticles at 18,000 rpm for 60 min at 4 °C). After purification, the supernatant liquid was discarded and the noisome sediment containing loaded AgNPs was dissolved and diluted, and the amount of Ag loaded in the noisome system was determined by ICP-MS method. Finally, using the required concentrations and the following formula, the encapsulation efficiency of AgNPs in niosomes was calculated 20,21 .

$$encapsulation\ efficiency\ (\%) = \frac{\text{Amount of silver encapsulated inside niosomes}}{\text{Initial amount of added silver}} \times\ 100$$

Investigation of cytotoxicity

The cytotoxic properties of AgNPs and niosome formulations were thoroughly evaluated against the normal human lung cell line MRC5(were procured from the Pasteur Institute of Iran, a renowned research institution in the Middle East). In this experimental framework, MRC5 cells were inoculated in a 96-well plate at a density

of 2×10^4 cells per well and were incubated until achieving an optimal confluence of approximately 70%. Subsequently, the cell culture medium was replaced with a fresh medium incorporating Nio-AgNPs at various concentrations (expressed in μ g/ml) and incubated for a period of 5 h. Following this incubation interval, the culture medium was discarded and substituted with fresh medium, which was then incubated for an additional 24 h. Thereafter, the MTT assay was performed to quantitatively evaluate cell viability and to elucidate the cytotoxic effects that were observed¹⁹.

Investigation of toxicity on cancer cells in presence and absence of radiation

The cytotoxic potential of synthetic formulations was systematically assessed utilizing differing concentrations of AgNPs, niosomes, and Nio-AgNPs on the A549 (were procured from the Pasteur Institute of Iran, a renowned research institution in the Middle East) cancer cell line using the MTT method. In this experimental setup, A549 cells were seeded in a 96-well plate at a density of 1×10^4 cells per well and incubated until an appropriate density was reached (approximately 70%). Subsequently, the cell culture medium was exchanged for a new medium containing the synthesized nanoparticles and incubated for 5 h. After this period, the culture medium was removed and replaced with fresh medium, where in one of the plates was subjected to X-ray exposure (4 Gy and 6 mV) while the other plate was maintained as a control (without radiotherapy), followed by an additional incubation period of 24 h. Then MTT test steps were performed to measure the cell viability and evaluate the effects of cytotoxicity. For X-ray radiation, a Siemens Primus model linear accelerator was used, which operates at a voltage of 6 mV. The samples were placed in the X-ray instrument cabinet and exposed to radiation 19 .

Statistical test

In this study, statistical analysis was performed using Prism GraphPad 8 software. Variance used to compare the difference between different treatments with the control group. The results were reported as mean \pm SD. In all comparisons, P-value less than 0.05 were reported as a sign of significance.

Results

Synthesis of AgNPs, niosomes and Nio-AgNPs

Different formulations, including AgNPs, niosomes and AgNPs, niosomes, and Nio-AgNPs, were used as radiosensitizers for the treatment of lung cancer in the presence and absence of Radiotherapy. AgNPs were synthesized using the Frenz method and sodium citrate reduction. Next, niosomes and Nio-AgNPs were prepared using the hydration method, using water and water containing synthesized AgNPs, respectively.

Characterization

Investigating the properties of nanoparticles is a branch of nanometerology that describes or measures the physical and chemical properties of nanoparticles. In fact, the characterization of nano materials is the determination of various characteristics of nanostructures, including particle size, particle shape, optical properties, mechanical properties, surface charge, etc. To determine each of the mentioned characteristics, special tools and techniques are used, which give us accurate and useful information from nano dimensions. Since the unique properties of nanomaterials are highly dependent on the particle size, surface structure and interactions between their constituent particles, therefore, the characterization of nanomaterials is very important in the development and application of nanomaterials.

Determining the size and dispersion index of nanoparticles

The results obtained from the DLS device for each of the formulations are shown in Fig. 1(A-E). Based on the results, the average hydrodynamic diameter of the samples for AgNPs is 55.81 ± 0.26 nm, niosome is 156.3 ± 3.51 nm, and Nio-AgNPs is 163.1 ± 1.21 nm. The PDI of the prepared nanoparticles was 0.287 ± 0.00 , 0.367 ± 0.00 , and 0.281 ± 0.00 for AgNPs, niosomes, and Nio-AgNPs, respectively.

Optical properties of prepared formulations

The optical properties of the synthesized nanosystems investigated by UV-Vis spectroscopy. From the results obtained in Fig. 2a, the absorption peak λ max of AgNPs was observed at the wavelength of 438 nm. The scanning results for the niosome in the wavelength range of 350–600 nm also showed that the niosome has no peak in this range. The comparison of UV-Vis spectra related to niosomes, AgNPs and Nio-AgNPs indicates that the characteristic peak related to AgNPs is observed with a slight shift after loading inside the niosomes (Fig. 2a). the obtained results clearly confirm the successful loading of AgNPs inside niosomal formulations.

Investigating the chemical structure of nanosystems

The composition and chemical architecture of the synthesized nanoparticles were systematically assessed utilizing the FT-IR technique, with the outcomes depicted in Fig. 2b. In this illustration, the prominent absorption peak observed at 3402 cm⁻¹ is attributable to the presence of hydroxyl functional groups. The dual peaks observed at 2892 and 2921 cm⁻¹ are associated with the symmetric and asymmetric stretching vibrations of methylene functional groups present in the organic compounds employed in the synthesis of AgNPs, specifically those citrate ions that are adsorbed onto the surface, alongside the niosomes comprising Span 80, Tween 80, and cholesterol. The distinctive peaks located at 1733 cm⁻¹ are indicative of the functional groups corresponding to aldehydes and esters within the molecular framework of Span 80 and Tween 80^{22,23}. The absorption peak identified at 1580 cm-1 signifies the stretching of the carbon-carbon (C-C) bond, as well as the bending vibrations of hydroxyl groups. The FTIR spectral analysis of silver nanoparticles (AgNPs) (Fig. 2b) revealed a variety of peaks at approximately 3433, 2931, 1596, 1350, 921, 779, 612, and 514 cm⁻¹, which appear to correlate with the citrate ions that are adsorbed onto the surface of AgNPs during the synthesis phase. Through comparative

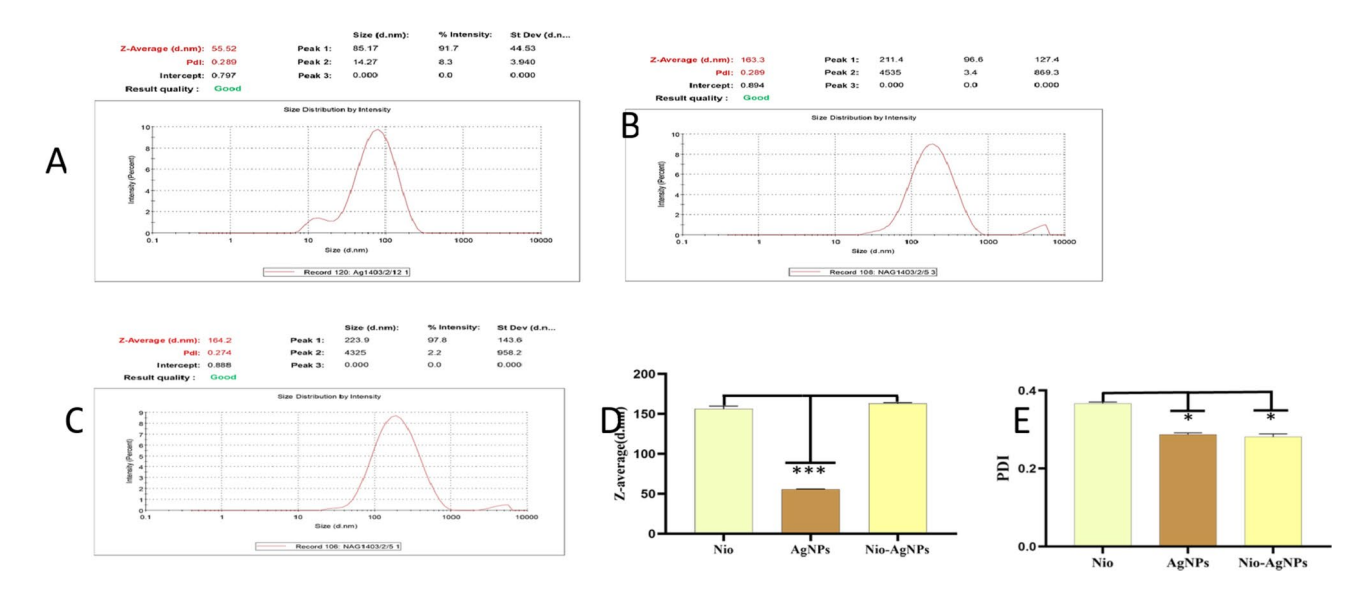
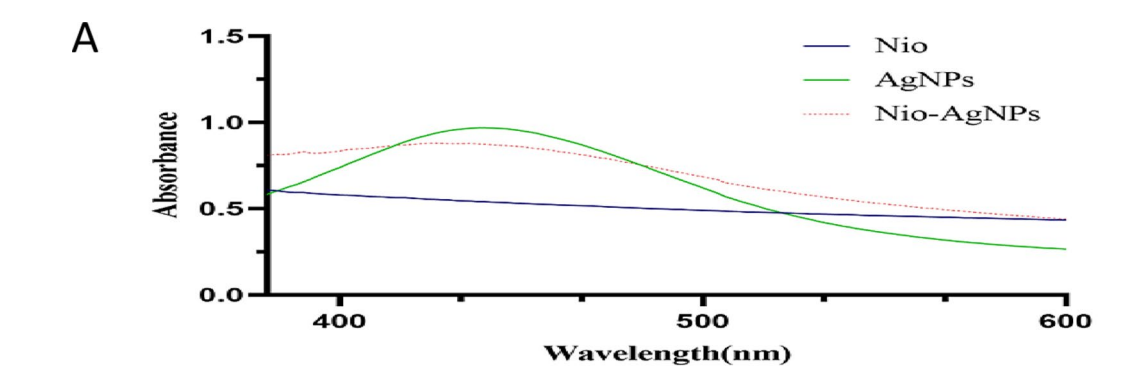


Fig. 1. DLS image related to the size of nanoparticles. **(A)** DLS image related to the size of AgNPs, **(B)** DLS image related to the size of niosomes, **(C)**, DLS image related to the size of Nio-AgNPs. **(D)**, Average size of niosomes (Nio), AgNPs, and Nio-AgNPs. $(P < 0.001 \neg^{***})$. **(E)**, Poly dispersity index (PDI) of niosomes (Nio), AgNPs, and Nio-AgNPs. $(P < 0.0179 \neg^*)$



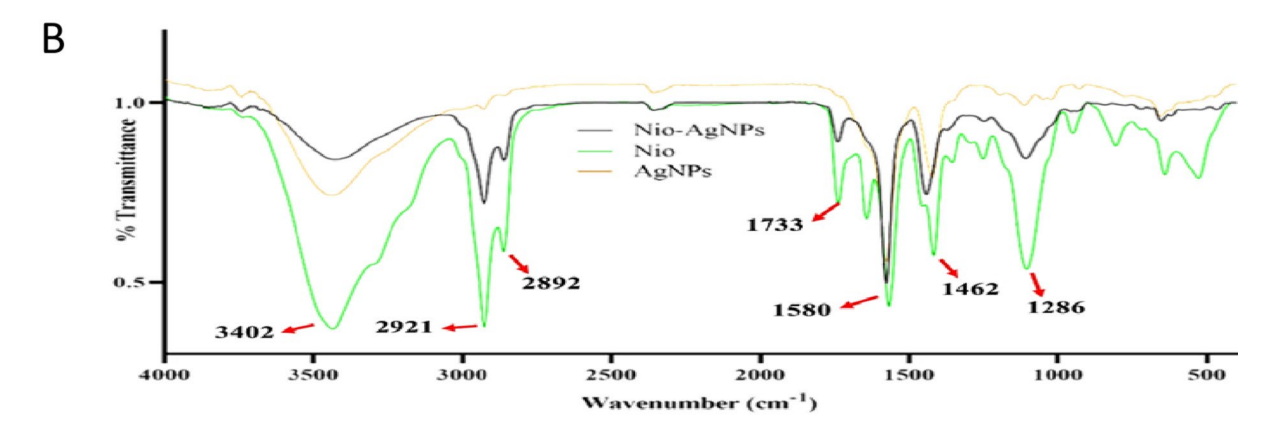


Fig. 2. (A) UV-Vis spectra of formulations of niosomes (Nio), AgNPs, and Nio-AgNPs. (B) FTIR spectra of of plain niosomes (Nio), AgNPs, and Nio-AgNPs.

analysis of the FT-IR spectra of niosomes, AgNPs, and Nio-AgNPs, it is observed that the characteristic peaks of Ag exhibit slight shifts in the final formulation, thereby confirming the successful encapsulation of AgNPs within the niosomal structures at 934, 519, 621, and 769 cm⁻¹²⁴.

Investigating the morphology of nanparticles

The morphological characteristics of the prepared nanoparticles were investigated by FE-SEM technique. The images obtained in Fig. 3a show that the prepared niosomes containing AgNPs are spherical, uniform and with smooth surfaces. In the following, EDAX analysis method was used for element analysis. The results of Linescan and Mapping methods are shown in Fig. 3b. Using the results shown in Fig. 3c and the weight percentages of each of the studied elements (carbon, nitrogen, oxygen, and silver) in Table 1, it can be concluded that AgNPs are successfully incorporated into niosomes structures.

Determination of concentration and encapsulation efficiency

Determining of the concentration and encapsulation efficiency of AgNPs inside niosomes using the ICP-MS method showed the encapsulation efficiency of $49.9\pm0.40\%$. Noisome containing AgNPs are compared with other noisome are shown in Table 2.

Determining the toxicity of synthesized nanosystems

Determination of toxicity on normal cells

Cytotoxicity of AgNPs and niosomes containing AgNPs on MRC-5 cell line was investigated using MTT test. The obtained results are given in Fig. 4a. As it has shown, the control group showed 100% cell viability. However, cell viability has decreased in the case of AgNPs in a dose-dependent manner. This means that AgNPs showed a toxic effect in high concentrations. However, it is known that the loading of AgNPs inside the niosomal carriers increased the cell viability and covered the toxicity of AgNPs. Therefore, the results obtained from this section showed that the prepared niosomal nanoparticles successfully reduce the toxicity effect of AgNPs on normal cells.

Results of cell viability test with MTT test

The MTT assay was utilized to assess the cytotoxicity of AgNPs and niosomes containing AgNPs against the human lung cancer cell line (A549) at three distinct concentrations of 2.5 μ g/mL, 5 μ g/mL, and 10 μ g/mL, both in the absence and presence of X-ray radiation (administered at a dose of 4 Gy). As illustrated in Fig. 4b, the control group devoid of nanoparticles (comprising solely the culture medium) exhibited a cell viability rate of 100%. Nevertheless, the therapeutic efficacy of AgNPs demonstrated an enhancement correlating with the elevation in concentration. The cell population subjected to irradiation at a dose of 4 Gy (Gy) manifested approximately 77.53% cell viability. The survival rate of cells treated with AgNPs at a concentration of 2.5 μ g/mL in conjunction with radiation was estimated to be around 83%. The viability of cells exposed to AgNPs and niosomes containing AgNPs at a concentration of 10 μ g/mL in the presence of radiation was observed to decline to 59% and 46%, respectively. These findings unequivocally indicate that the nanoparticles synthesized in this investigation exhibited superior therapeutic effects relative to the group that received solely X-ray radiation, thereby signifying an augmentation in radiation sensitivity attributable to the nanoparticles. The survival of cells treated with niosomes containing AgNPs in combination with X-ray radiation demonstrated the most pronounced decrease when compared to other experimental conditions.

The results of determining the synergistic combination of nanoparticles with radiotherapy

Analysis of the isobologram plot was used for the combined effect of the final formulation, i.e. niosomes containing AgNPs with radiation. The combined index (CI) of niosomes containing silver nanoparticles and radiotherapy was determined using the method described by Chou-Talalay. Based on the Chou-Talalay equation, CI < 1 indicates a synergistic effect, CI > 1 indicates antagonism effect, and CI = 1 indicates an additive effect. The results obtained in Fig. 4c and d; Table 3 showed that the combined index for niosomes containing AgNPs prepared along with radiotherapy is below one, which indicates the synergist effect.

Discussion

Radiotherapy represents a critical intervention in the management of cancer, particularly in the case of lung cancer. Approximately 77% of individuals diagnosed with lung cancer exhibit a clinical justification for the utilization of radiotherapy. Non-small cell lung cancer (NSCLC), which accounts for the predominant proportion of lung cancer cases, encompasses histological subtypes such as squamous cell carcinoma, adenocarcinoma, and large cell carcinoma⁶. Radiotherapy serves as a fundamental component in the therapeutic regimen for numerous malignancies, including NSCLC. The pursuit of strategies to amplify the efficacy of radiotherapy in eradicating tumor cells while concurrently safeguarding healthy tissues is an area of considerable scholarly interest. A methodical approach to surmount these obstacles involves the incorporation of radiosensitizers, which are specifically formulated to enhance the effectiveness of radiotherapy while mitigating adverse effects on non-cancerous tissue. The concept of augmenting the susceptibility of tumors to radiation-induced damage is referred to as radiation sensitivity, with radiosensitizers functioning as agents that potentiate the impact of radiation on neoplastic cells¹⁰. The foundational tenet of radiotherapy entails the engagement of ionizing radiation with components of tumor cells, either directly or indirectly. Direct engagement results in the compromise of essential biological macromolecules, including nucleic acids and proteins, thereby obstructing cellular division and proliferation, ultimately culminating in cellular apoptosis. Conversely, in the context of indirect interaction, radiation catalyzes the formation of reactive oxygen species (ROS) and free radicals, which perturb biological molecules⁶. Among the diverse array of nanoparticle systems, metallic nanoparticles, such

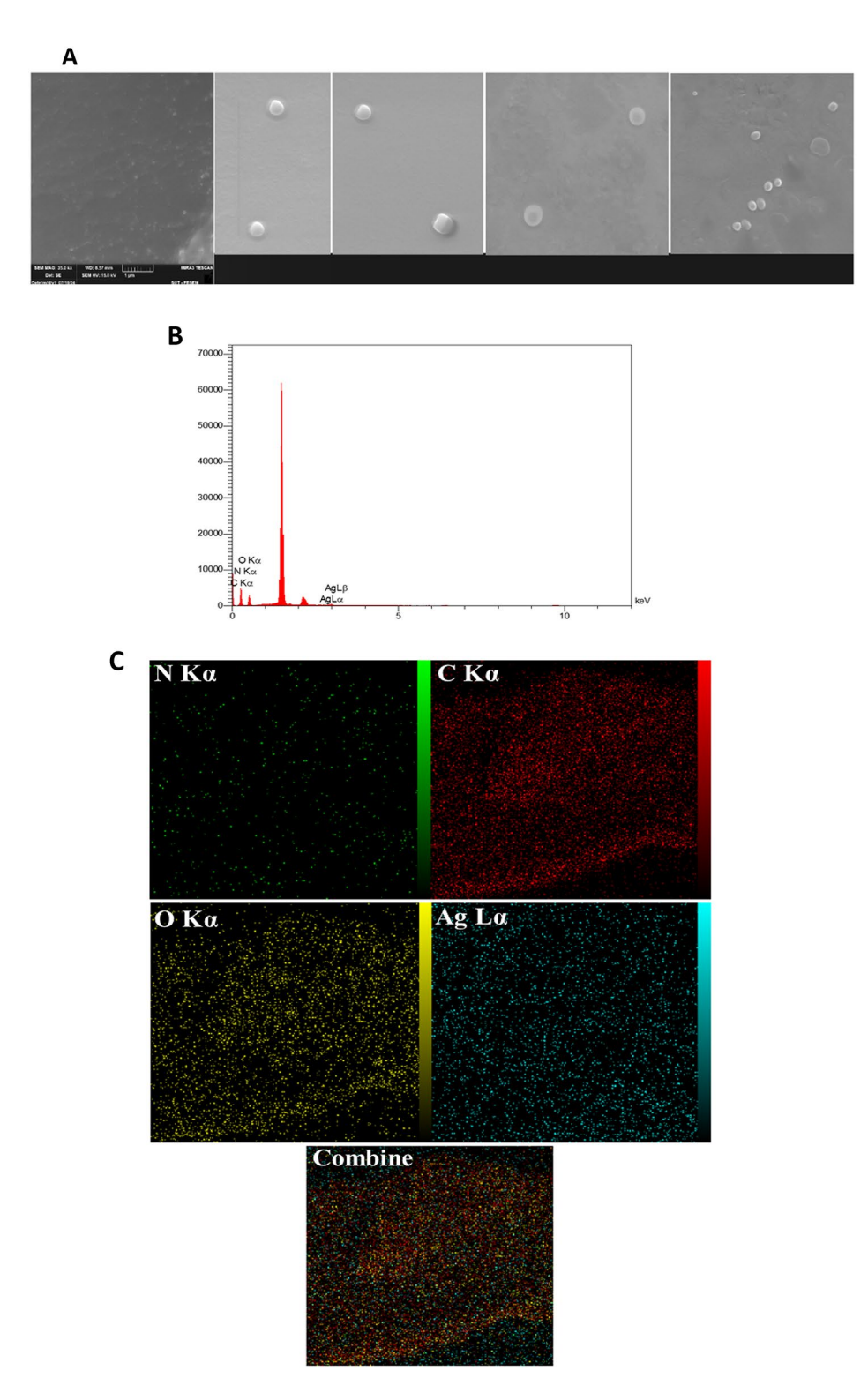


Fig. 3. (**A**) FE-SEM images of the niosomes containing AgNPs. (**B**) Linescan results obtained for niosomes containing AgNPs from EDAX technique (C), Mapping results obtained for niosomes containing AgNPs from EDAX technique.

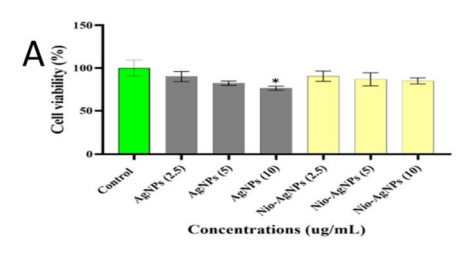
as silver nanoparticles and gadolinium nanoparticles, have emerged as promising candidates in the domain of NSCLC radiosensitization. In this context, Gowda et al. demonstrated that AgNPs significantly curtailed the expression of X-ray-induced epithelial-mesenchymal transition markers in A549 cells, including Vimentin and N-cadherin, while concurrently enhancing the expression of E-cadherin, a modification that ultimately diminishes the radioresistance of tumor cells²⁵. Additionally, Reetta et al. observed that AgNPs induce cell cycle

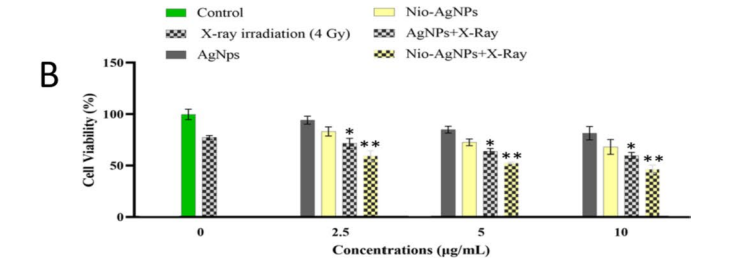
Elt	Line	Int	Error	K	Kr	W%	A%	ZAF	Pk/Bg	LConf	HConf
С	Ka	507.4	87.5808	0.5481	0.1844	36.63	45.04	0.5032	642.70	36.04	37.23
N	Ka	19.7	87.5808	0.0214	0.0072	5.22	5.50	0.1378	7.17	4.79	5.65
О	Ka	273.4	87.5808	0.3001	0.1009	52.80	48.73	0.1911	262.69	51.63	53.96
Ag	La	102.4	79.1951	0.1304 1.0000	0.0439 0.3364	5.35 100.00	0.73 100.00	0.8200	10.36	5.15	5.54

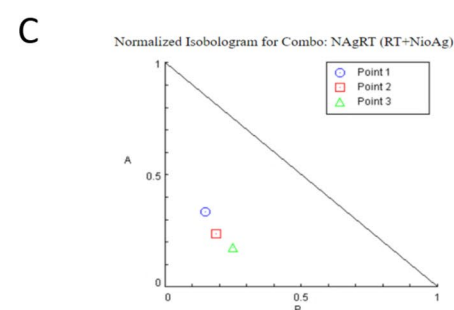
Table 1. Numerical results of carbon, nitrogen, oxygen and silver elements from EDAX analysis.

Nanoparticles	Size(nm)	PDI	Encapsulation efficiency %
Nio-AgNPs	163	0.281	49.9
Nio-AuNPs	127.8	0.430	57.04
Nio-ZnNPs	429.	0.313	15.56
Nio-AuNPs	153.6	0.242	59
Nio-SeNPs	137	0.211	37.58
Nio-AgNPs	251.7	0.4	4

Table 2. Noisome containing silver nanoparticles are compared with other niosome.







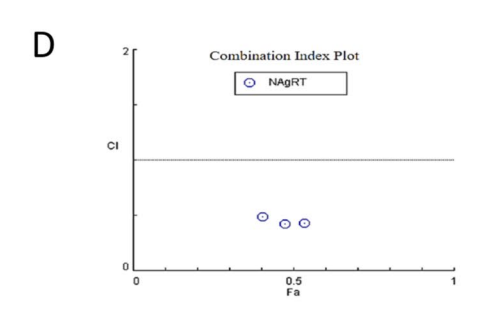


Fig. 4. (**A**) Cytotoxicity of AgNPs and niosomes containing AgNPs in different concentrations on normal cells. ($P < 0.0179 \neg^*$)The diagram of combined treatment in A549 cells prepared using Compusyn software. (**B**) Cytotoxicity of AgNPs and niosomes containing AgNPs in different concentrations on lung cancer cells. ($P < 0.0179 \neg^*$ and $P < 0.0028 \neg^{**}$), (**C**). Isobologram diagram of the combined effect of niosomes containing AgNPs and radiotherapy. (**D**) The diagram of combined treatment in A549 cells prepared using Compusyn software.

Radiotherapy dose	The dose of the Nio-AgNPs	CI	Effect
4/0	2.5	48,644/0	4057/0
4/0	5	42,589/0	475/0
4/0	10	42,763/0	5359/0

Table 3. Numerical results of investigating the combined effect of niosomes containing AgNPs and radiotherapy.

arrest at various phases(A549 and Calu-1 cells in G2 phase, BEAS-2B in S phase), resulting in elevated ROS production and increased protein oxidation within mitochondria. Consequently, the sensitivity of these cells to radiotherapy was heightened²⁶. Due to the capacity of nanoparticles to concentrate ionization energy within cancerous tumors, they augment the efficacy of radiation therapy. The influence of high atomic number (high Z) nanosensitizers is predicated on the photoelectric absorption properties of the material, which can facilitate the interaction of photons or electrons. Upon the application of radiation, a bound electron absorbs a photon, leading to its ejection from the particle. The phenomenon of photoelectric absorption is contingent upon the atomic number, thus elements with elevated Z are predisposed to enhanced radiation emission²⁷. AgNPs, like gold nanoparticles, have radiosensitizing properties. As with other high Z-number atoms, AgNPs use a similar mechanism of action for radio sensitization. AgNPs have a relatively lower price than gold nanoparticles and are therefore affordable, but they are relatively less biocompatible²⁸. In this context, we investigated the role of AgNPs loaded inside niosome carriers for use in radio sensitivity for lung cancer. For this purpose, at first AgNPs synthesized with chemical reduction method using sodium citrate and its physicochemical properties were investigated with different techniques. The hydrodynamic diameter and PDI for AgNPs were obtained as 55.81 ± 0.26 nm and 0.287, respectively. The size of AgNPs obtained according to the used synthesis method (Frenz method) was consistent with previous studies. In the study published by Miguel et al., the hydrodynamic diameter of AgNPs obtained by the Frenz method through DLS measurements was between 6 and 70 nm²⁹⁻³¹.

The optical properties of the AgNPs were investigated by UV-Vis spectroscopy and the absorption peak (\lambdamax) at the wavelength of 438 nm confirmed the successful synthesis of the resulting nanoparticles. The results obtained in this study showed a good agreement with the results reported in this field for the absorption peak observed at 438 nm^{32,33}. AgNPs are very efficient in absorbing and scattering the light. However, they are less biocompatible and pose significant challenges in terms of biocompatibility, immune response, and interaction with proteins during long-term exposure³⁴. On the other hand niosomes which are characterized by their bilayer lipid architecture, show biodegradability immunocompatibility, and preferential association with the plasma proteome³⁵. The low biocompatibility and stability of AgNPs limits their mass production and wide application. Using niosomes as a carrier to protect and cover AgNPs give a new perspective to solve these problems. Therefore, in the present study, niosomes containing AgNPs were prepared by thin layer hydration method and their properties were investigated in different ways. The results of hydrodynamic diameter and dispersion index for the resulting niosomes were 163.1 ± 1.21 nm and 0.281 nm respectively, which results are comparable with many studies published in this field. In a published study that synthesized niosomes containing selenium nanoparticles, the hydrodynamic size of the resulting niosomes was found to be 149.23±3.164³⁶. The poly dispersity index (PDI) within the realm of nanoparticle synthesis demonstrates a variable range, specifically from 0.01 (indicative of singularly dispersed particles) to values between 0.5 and 7.5; conversely, a PDI value exceeding 0.7 indicates a substantial distribution in particle size within the final formulations. The distribution of particle size is a critical determinant in assessing the functional efficacy of nanoparticles. The propensity of lipid-based nanocarriers to localize within the target tissues is contingent upon their physicochemical properties, which encompass particle size distribution. Consequently, the successful development of safe, stable, and effective nanocarriers necessitates the formation of homogenous (monodisperse) populations of nanocarriers characterized by specific dimensional attributes. In the present investigation, the PDI values recorded were 0.287 ± 0.00 , 0.367 ± 0.00 , and 0.281 ± 0.00 for AgNPs, niosomes, and Nio-AgNPs, respectively, with all samples exhibiting PDI values below 0.4. The PDI values obtained, ranging from 0.01 to 0.7, signify a narrow and homogeneous particle size distribution, leading to the conclusion that the PDI of all samples resides within an acceptable parameter³⁷.FE-SEM technique was used to determine the morphology of niosomes containing AgNPs. The obtained results showed that the prepared nanoparticles have a uniform morphology with spherical shapes. The results of FE-SEM analysis are consistent with the study published by Rinaldi et al.., who synthesized niosomes containing AgNPs, so that in their study, morphological investigations showed that niosomes are spherical in shape³⁸. DLS technique is mainly used to determine the size and size distribution of particles in aqueous or physiological solutions. The size obtained from DLS is usually larger than the FE-SEM technique, which may be due to the effect of Brownian motion. The data from UV-Vis and EDAX technique (Linescan and Mapping) confirmed the presence of AgNPs in niosomes. In the obtained UV-Vis spectra, the absorption peak related to AgNPs was observed with a slight shift in the formulation of Nio-AgNPs. In published researches, various methods have been used to determine the concentration of AgNPs, including atomic absorption spectroscopy (AAS), inductively coupled plasmaoptical emission spectroscopy (ICP-OES) and ICP-MS. One of the reasons why ICP-MS is so widely used to determine the concentration of AgNPs is that it provides very low detection limits for almost all the elements it can measure. ICP-MS can detect many elements at levels below 0.1 ppm as well^{34,39}. Although the AAS method provides good sensitivity, it is generally less sensitive than ICP-MS. Therefore, in the present study, the concentration of silver in AgNPs, niosomes containing AgNPs was determined by ICP-MS method, and with the amount of silver concentration, the percentage of Ag encapsulation inside niosomes were calculated. The results obtained in this field showed that AgNPs with encapsulation percentage equal to 0.40 ± 49.9% were placed inside the niosomes⁴⁰. Considering the different results that have been published about the safety and biocompatibility of nanomaterials in various previous studies, the validity of the analytical methods used for toxicity evaluation are really important. Therefore, the in vitro cytotoxicity evaluation of AgNPs as well as Nio-AgNPs was performed using the MTT test on normal lung cells (MRC-5). The findings of this evaluation showed that AgNPs in the studied concentrations (2.5, 5 and 10 µg/mL) caused dose-dependent toxicity for cells compared to the control group. However, when the designed nanoparticles were loaded inside niosomes, their toxicity decreased significantly. These results clearly showed the importance of niosomes in improving the biocompatibility of prepared formulations. Previous study has shown that AgNPs synthesized by chemical method were toxic on MRC-5 cells. In this study, the half-maximum inhibitory concentration (IC50) in 24-hour treatment on MRC-5 cells was reported as 31.5 µg/mL. Therefore, the toxicity of AgNPs on normal lung cells in our study is in

accordance with published studies in this field⁴¹⁻⁴⁴. In another research published in 2024, first zinc oxide nanoparticles and niosomes containing zinc oxide nanoparticles were synthesized. Cancer cell line (MDA-MB 361, MCF-7 and T47D) and normal cell line (HEK-293) were used to evaluate cell toxicity and compatibility. The obtained results showed that niosomes on normal and cancer cell lines have no significant toxicity up to a concentration of 1000 µg/ml. Zinc oxide nanoparticles caused toxicity on normal and cancer cell lines. The important point in this study was that niosomes containing zinc oxide nanoparticles caused a significant reduction in toxicity compared to zinc oxide nanoparticles only in front of the normal cell line, while in the cancer cell line they caused an increase in the toxicity of zinc oxide nanoparticles. This phenomenon may be perceived as an opportunity for niosomal carriers in the transport of metallic nanoparticles. A contributing factor to the cytotoxicity associated with niosomes encapsulating oxide nanoparticles was the regulated and targeted release of the therapeutic agent into the cellular environment³⁵. Haddadian et al. conducted a comparative analysis of the effects of selenium nanoparticles encapsulated within niosomes versus those of free selenium nanoparticles. Their findings indicated that the incorporation of selenium nanoparticles into niosomes augmented their anti-cancer efficacy, attributable to the targeted delivery of the therapeutic agent into the cells⁴⁵. Similarly, Rezaei et al. assessed and contrasted the cytotoxic effects of gold nanoparticles encapsulated in niosomes against their free counterparts in cancer cell lines. The outcomes of this investigation revealed that the IC50 value for niosomes was significantly lower than that of the free nanoparticles (specifically $2.62 \pm 200 \,\mu g/mL$ compared to 3.25 ± 155 µg/mL), thereby demonstrating an enhancement in the anticancer properties of niosomes containing gold nanoparticles⁴⁶. The cytotoxicity exhibited by AgNPs is contingent upon an array of factors including morphological characteristics, dimensional parameters, surface area, surface chemistry, concentration levels, lateral dimensions, surface architecture, functional moieties, purity, and the presence of associated proteins. Research indicates that AgNPs possess the capability to induce cytotoxic effects in mammalian cancer cells at concentrations ranging from 2 to 100 micrograms per milliliter. In a peer-reviewed investigation, A549 cancer cells were subjected to varying dimensions of silver nanoparticles (20-40 nm) at concentrations of 2-10 μM over a duration of 24 h. Noteworthy indicators of toxicity were recorded for AgNPs even at the maximal dosage administered. In this particular framework, pronounced cytotoxicity was identified at concentrations exceeding 4 µM, with AgNPs demonstrating a dose-dependent modulation of cellular viability⁴⁷. Within the confines of the current research, AgNPs elicited a dose-dependent toxic response in the lung cancer cell line, thereby corroborating the observed dose-dependent inhibitory effects. The observed discrepancies in toxicity relative to other investigations are ascribed to the variations in the size of AgNPs as well as the duration of cellular exposure. The effect of different doses of X-rays (2, 4 and 6 Gy) on A549 cell line was investigated in the previous research. The findings showed that the prescribed doses cause significant cytotoxicity and the 4 Gy dose showed a significant effect in the treatment of cancer cells. Therefore, in the present study, the effect of a 4 Gy dose of radiation along with AgNPs in lung cancer treatment was investigated. The results obtained in this study are consistent with the results reported by other research groups in this field. Barlas et al.. found that radiotherapy doses significantly damage A549 cells^{37,48,49}. It is necessary to remember that the position of cells in the cell cycle is an intrinsic vital factor that modulates cell sensitivity to radiotherapy. Generally, cells at the end of G1 phase and during S phase showed radiation resistance, while cells in G2 phase and cells undergoing mitosis show more sensitivity to radiation. Cells may show more radiation resistance at the beginning of G1 phase. However, this dependence on the cell cycle phase is different for different types of cells⁵⁰.

Conclusion

In the present study, the development of niosomal containing AgNPs was carried out through the thin layer hydration method to evaluate the effectiveness of cancer radiotherapy in the presence of these synthesized nanoparticles. FT-IR, UV-Vis, DLS, FE-SEM and EDAX techniques were used to analyze the physical and chemical properties of nanoparticles. The results of the cytotoxicity test showed that niosomes containing AgNPs against the MRC-5 cell line at different concentrations reduce the toxicity of loaded AgNPs and were introduced as a suitable option for cell tests. The results obtained from the MTT and CI index tests showed that the synthesized formulation, in combination with radiotherapy, increases the efficiency of radiotherapy and creates a synergistic effect. In particular, the use of niosomal carrier was effective in improving the efficiency of AgNPs in increasing cytotoxicity on A549 cell line and at the same time, it reduced the toxicity of AgNPs in MRC-5 cell line. Our team showed the importance of using niosomal carriers in enhancing the performance of AgNPs in radiotherapy treatments. In conclusion we could show that niosomal nanocarriers containing AgNPs were able to increase the efficiency of radiotherapy against A549 cancer cells in laboratory conditions.

Limitations and future prospect

Our study was limited to investigating the effect of AgNPs in a specific cell line. To achieve more comprehensive and generalize results, it is suggested that future research include more diverse cell lines. The use of different cell lines can help identify differences in cell response to treatment and evaluate the effectiveness of nanoparticles in different conditions. This approach can lead to a better understanding of the mechanisms of the effect of nanoparticles on different types of cells and the identification of cell lines with different sensitivity or resistance. Considering that in vitro and in vivo condition have fundamental differences, it is necessary to investigate the effect of AgNPs loaded in niosomes in in vivo models as well. Evaluating the effects of nanoparticles in living models can help to better understand their behavior in the complex conditions of the human body, including absorption, distribution and toxicity in different organs. These more comprehensive assessments can provide more accurate information for clinical applications and optimization of nano medicine treatments. The effect of radiotherapy on cells strongly depends on cell cycle. For this reason, it is important to examine the cell cycle as a key parameter in future studies. Assessing the state of cells in different stages of the cell cycle can help

to better understand how they interact with radiotherapy and nanoparticles and lead to the optimization of treatment strategies. Investigating the effects of nanoparticles in different stages of the cell cycle can provide valuable information about the mechanisms of DNA damage and repair, as well as the synergistic mechanisms of nanoparticles with radiotherapy. As a result, a significant limitation of the current research is the lack of analysis of cell cycle stages, which prevents a deeper understanding of the effect of cell cycle stages on the effectiveness of radiation therapy. Moreover; the other limitation of the present study is that this study only evaluated cell viability and apoptosis, and other tests such as production of reactive oxygen species (ROS), oxidative stress, initiation of DNA damage, and effects on the cell cycle did not investigate. Thus, it needs more research to investigate DNA repair, cell cycle arrest and cell aging in relation to X-ray radiation and treatment with niosomes containing AgNPs. It is also better to investigate the condition in vitro and in vivo using a wider range of concentrations and different treatment times are necessary to better understand the effects and optimize the treatment.

Data availability

Data availability The datasets used during the current study available from the corresponding author on reasonable request.

Received: 22 February 2025; Accepted: 22 April 2025

Published online: 29 April 2025

References

- 1. Li, Y. et al. CircMYBL1 suppressed acquired resistance to osimertinib in non-small-cell lung cancer. Cancer Genet. Volumes 284-285, Pages 34-42. (2024).
- 2. Cao, Z. et al. Comprehensive pan-cancer analysis reveals ENC1 as a promising prognostic biomarker for tumor microenvironment and therapeutic responses. Sci. Rep. 14, 25331 (2024).
- 3. Hirsch, F. R. et al. Lung cancer: current therapies and new targeted treatments. Lancet 389 (10066), 299-311 (2017).
- 4. Moradi, A., Esmaeilzadeh, A. & Elahi, R. Melatonin as a novel candidate for gene therapy of atherosclerosis. Atherosclerosis 3 (1), 1027 (2020).
- 5. Mohammadi, V. et al. Chimeric antigen receptor (CAR)-based cell therapy for type 1 diabetes mellitus (T1DM); current progress and future approaches. Stem Cell. Reviews Rep. 20 (3), 585-600 (2024).
- 6. Uzel, E. K., Figen, M. & Uzel, Ö. Radiotherapy in lung cancer: current and future role. Sisli Etfal Hastan Tip Bul. 53 (4), 353 (2019).
- 7. Elahi, R. et al. Targeting the cGAS-STING pathway as an inflammatory crossroad in coronavirus disease 2019 (COVID-19). Immunopharmacol. Immunotoxicol. 45 (6), 639-649 (2023).
- 8. Wang, Y. et al. Tumor Cell-Targeting and tumor Microenvironment-Responsive nanoplatforms for the multimodal Imaging-Guided photodynamic/photothermal/chemodynamic treatment of cervical Cancer. Int. J. Nanomed. 19, 5837-5858 (2024).
- 9. Babaei, M. & Ganjalikhani, M. The potential effectiveness of nanoparticles as radio sensitizers for radiotherapy. BioImpacts: BI. 4 (1), 15 (2014).
- 10. Kwatra, D., Venugopal, A. & Anant, S. Nanoparticles in radiation therapy: a summary of various approaches to enhance radiosensitization in cancer. Translational Cancer Res. ;2(4). (2013).
- 11. Arif, M. et al. Nanotechnology-based radiation therapy to cure cancer and the challenges in its clinical applications. Heliyon; 9(6).
- 12. Matysiak-Kucharek, M., Sawicki, K. & Kapka-Skrzypczak, L. Effect of silver nanoparticles on cytotoxicity, oxidative stress and proinflammatory proteins profile in lung adenocarcinoma A549 cells. Ann. Agric. Environ. Med. 30 (3), 566-569 (2023)
- 13. Abdellatif, A. A. H. et al. Exploring the green synthesis of silver nanoparticles using natural extracts and their potential for cancer treatment. 3 Biotech. 14, 274 (2024).
- 14. Allen, C., Her, S. & Jaffray, D. A. Radiotherapy for cancer: present and future. pp. 1-2. (2017).
- 15. Ag Seleci, D., Seleci, M., Walter, J-G., Stahl, F. & Scheper, T. Niosomes as nanoparticular drug carriers: fundamentals and recent applications. J. Nanomaterials. 2016 (1), 7372306 (2016).
- 16. Kerr, D., Rogerson, A., Morrison, G., Florence, A. & Kaye, S. Antitumour activity and pharmacokinetics of niosome encapsulated adriamycin in monolayer, spheroid and xenograft. Br. J. Cancer. 58 (4), 432-436 (1988).
- 17. -Ghafarlou, M. et al. Bovine serum albumin-mediated synthesis and quorum sensing inhibitory properties of Ag-Ag2S nanoparticles. Nanomedicine 17 (28), 2145-2155 (2022).
- -Mousazadeh, N. et al. Anticancer evaluation of methotrexate and curcumincoencapsulated niosomes against colorectal cancer cell lines. Nanomed. (Lond). 17 (4), 201-217. 10.2 217/nnm-2021-0334 (2022)
- -Taheri, R. A. et al. Niosomes loaded with gold nanoparticles for enhanced radiation therapy in lung cancer. Nanomedicine 19 (27), 2257-2270 (2024).
- 20. -Mohamed, H. B. et al. Niosomes: a strategy toward prevention of clinically significant drug incompatibilities. Sci. Rep. 7 (1), 6340 (2017).
- 21. Demir, B. et al. Theranostic niosomes as a promising tool for combined therapy and diagnosis: all-in-one approach. ACS Appl. Nano Mater. 1 (6), 2827-2835. https://doi.org/10.1021/acsanm.8b0 (2018).
- 22. Rehman, M. U. et al. Development of Niosomal formulations loaded with cyclosporine A and evaluation of its compatibility. Trop. J. Pharm. Res. 17 (8), 1457-1464 (2018).
- 23. Biswas, S. & Mulaba-Bafubiandi, A. F. Optimization of process variables for the biosynthesis of silver nanoparticles by Aspergillus Wentii using statistical experimental design. Adv. Nat. Sci. NanoSci. NanoTechnol. 7 (4), 045005 (2016).
- 24. Bhattacharjee, S., Debnath, G., Das, A. R., Saha, A. K. & Das, P. Characterization of silver nanoparticles synthesized using an endophytic fungus, penicillium oxalicum having potential antimicrobial activity. Adv. Nat. Sci. NanoSci. NanoTechnol. 8 (4), 045008 (2017).
- 25. Gowda, S. S. et al. Gallic acid-coated sliver nanoparticle alters the expression of radiation-induced epithelial-mesenchymal transition in non-small lung cancer cells. Toxicol. In Vitro. 52, 170-177 (2018).
- 26. Holmila, R. J. et al. Silver nanoparticles induce mitochondrial protein oxidation in lung cells impacting cell cycle and proliferation. Antioxidants 8 (11), 552 (2019).
- 27. Le Sech, C. et al. Comment on 'therapeutic application of metallic nanoparticles combined with particle-induced x-ray emission effect'. Nanotechnology 23 (7), 078001 (2012).
- Ma, J. et al. Nanoparticle surface and nanocore properties determine the effect on radiosensitivity of cancer cells upon ionizing radiation treatment. J. Nanosci. Nanotechnol. 13 (2), 1472-1475 (2013).
- Gakiya-Teruya, M., Palomino-Marcelo, L. & Rodriguez-Reyes, J. C. F. Synthesis of highly concentrated suspensions of silver nanoparticles by two versions of the chemical reduction method. Methods Protocols. 2 (1), 3 (2018).

- 30. Sadan, M. et al. Can silver nanoparticles stabilized by Fenugreek (Trigonella Foenm -graecum) improve tibial bone defects repair in rabbits? A preliminary study. *Open. Vet. J.* **14** (5), 1281–1293. https://doi.org/10.5455/OVJ.2024.v14.i5.23 (2024).
- 31. Abdellatif, A. A. H. et al. Silver citrate nanoparticles inhibit PMA-Induced TNFα expression via deactivation of NF-κB activity in human Cancer Cell-Lines, MCF-7. *Int. J. Nanomed.* **15**, 8479–8493 (2020).
- 32. Du, J. et al. Biosynthesis of large-sized silver nanoparticles using Angelica Keiskei extract and its antibacterial activity and mechanisms investigation. *Microchem. J.* 147, 333–338 (2019).
- 33. Huq, M. A. Biogenic silver nanoparticles synthesized by Lysinibacillus xylanilyticus MAHUQ-40 to control antibiotic-resistant human pathogens Vibrio parahaemolyticus and Salmonella Typhimurium. Front. Bioeng. Biotechnol. 8, 597502 (2020).
- 34. Berking, B. B., Mallen-Huertas, L., Rijpkema, S. J. & Wilson, D. A. Porous polymersomes as carriers for silver nanoparticles and nanoclusters: advantages of compartmentalization for antimicrobial usage. *Biomacromolecules* 24 (12), 5905–5914 (2023).
- 35. Rezaei, H., Iranbakhsh, A., Sepahi, A. A., Mirzaie, A. & Larijani, K. Formulation, Preparation of niosome loaded zinc oxide nanoparticles and biological activities. Sci. Rep. 14 (1), 16692 (2024).
- 36. Gharbavi, M. et al. Hybrid of niosomes and bio-synthesized selenium nanoparticles as a novel approach in drug delivery for cancer treatment. *Mol. Biol. Rep.* 47, 6517–6529 (2020).
- 37. Leiser, D. et al. Role of caveolin-1 as a biomarker for radiation resistance and tumor aggression in lung cancer. *PLoS One.* **16** (11), e0258951 (2021).
- 38. Rinaldi, F. et al. Hydrophilic silver nanoparticles loaded into niosomes: Physical-chemical characterization in view of biological applications. *Nanomaterials* **9** (8), 1177 (2019).
- Zanoni, I. et al. Use of single particle ICP-MS to estimate silver nanoparticle penetration through baby Porcine mucosa. Nanotoxicology 15 (8), 1005-1015 (2021).
- 40. Ayyanaar, S. & Kesavan, M. P. One-pot biogenic synthesis of gold nanoparticles@ saponins niosomes: sustainable nanomedicine for antibacterial, anti-inflammatory and anticancer therapeutics. *Colloids Surf., A.* **676**, 132229 (2023).
- 41. Ali, A. R., Anani, H. A. & Selim, F. M. Biologically formed silver nanoparticles and in vitro study of their antimicrobial activities on resistant pathogens. *Iran. J. Microbiol.* **13** (6), 848 (2021).
- 42. Abdellatif, A. A. H. et al. Exploring the green synthesis of silver nanoparticles using natural extracts and their potential for cancer treatment. 3 Biotech. 14, 274. https://doi.org/10.1007/s13205-024-04118-z (2024).
- 43. Abdellatif, A. A. H. et al. Green synthesized silver nanoparticles using the plant-based reducing agent Matricaria chamomilla induce cell death in colorectal cancer cells. Eur. Rev. Med. Pharmacol. Sci. 27 (20), 10112–10125. https://doi.org/10.26355/eurrev_202310_34191 (2023).
- 44. Abdellatif, A. A. H. et al. Bouazzaoui green synthesis of silver nanoparticles reduced with Trigonella foenum-graecum and their effect on tumor necrosis factor-α in MCF7 cells. Eur. Rev. Med. Pharmacol. Sci. 26 (15), 5529–5539 (2022).
- 45. Haddadian, A. et al. Niosomes-loaded selenium nanoparticles as a new approach for enhanced antibacterial, anti-biofilm, and anticancer activities. Sci. Rep. 12 (1), 21938 (2022).
- 46. Amale, F. R. et al. Gold nanoparticles loaded into niosomes: A novel approach for enhanced antitumor activity against human ovarian cancer. Adv. Powder Technol. 32 (12), 4711–4722 (2021).
- 47. Gurunathan, S., Kang, M. & Kim, J-H. Combination effect of silver nanoparticles and histone deacetylases inhibitor in human alveolar basal epithelial cells. *Molecules* 23 (8), 2046 (2018).
- 48. Zheng, H. et al. Inhibition of mTOR enhances radiosensitivity of lung cancer cells and protects normal lung cells against radiation. *Biochem. Cell Biol.* **94** (3), 213–220 (2016).
- 49. Barlas, F. B. et al. Multimodal theranostic assemblies: double encapsulation of protoporphyrine-IX/Gd 3+in niosomes. *RSC Adv.* **6** (36), 30217–30225 (2016).
- 50. Hill, I. E. et al. Understanding radiation response and cell cycle variation in brain tumour cells using Raman spectroscopy. *Analyst* **148** (11), 2594–2608 (2023).

Acknowledgements

This work was supported by the Deputy of Research of Zanjan University of Medical Sciences [A-12-430-64, ethical code: IR. ZUMS. BLC.1401.016].

Author contributions

Author contribution statementHossein Danafar: Supervision. Mahdi Nayyeri Maleki: Formal analysis. Amir Hosein Moradi: Methodology. Ali Sharafi: Project administration.: Kayvan Nedaei: Methodology.

Declarations

Competing interests

The authors declare no competing interests.

Ethical considerations

This study was approved by the Ethics Committee of the Zanjan University of Medical Sciences with IR.ZUMS. BLC.1401.016 ethical code, and the study participants signed an informed consent. All methods were carried out in accordance with Ethics Committee of the Zanjan University of Medical Sciences guidelines and regulations. All experimental protocols were approved by Zanjan University of Medical Sciences and licensing committee.

Additional information

Correspondence and requests for materials should be addressed to H.D.

Reprints and permissions information is available at www.nature.com/reprints.

Publisher's note Springer Nature remains neutral with regard to jurisdictional claims in published maps and institutional affiliations.

Open Access This article is licensed under a Creative Commons Attribution-NonCommercial-NoDerivatives 4.0 International License, which permits any non-commercial use, sharing, distribution and reproduction in any medium or format, as long as you give appropriate credit to the original author(s) and the source, provide a link to the Creative Commons licence, and indicate if you modified the licensed material. You do not have permission under this licence to share adapted material derived from this article or parts of it. The images or other third party material in this article are included in the article's Creative Commons licence, unless indicated otherwise in a credit line to the material. If material is not included in the article's Creative Commons licence and your intended use is not permitted by statutory regulation or exceeds the permitted use, you will need to obtain permission directly from the copyright holder. To view a copy of this licence, visit https://creativecommons.org/licenses/by-nc-nd/4.0/.

© The Author(s) 2025